ECOLE
SUPERIEURE
D'ÉLECTRICITÉ
Supélec
ELECTROMAGNETICS DEPARTMENT

SSN 417

Gif, January 13, 1998

Dr.C.Baum

Dear Dr.Baum,

Please, find here enclosed a new version of our manuscript entiteld:

"Spherical Near-Field Facility for Microwave Coupling Assessments in the 100 MHz - 6 GHz Frequency range" by D.Sérafin et al.

The first page has been remodeled, the pagination has been centered according to your recommandations. Furthermore, I made my best to improve the quality of the bad figures or in providing the originals.

The fax number you have used is wrong. Please note the right one below.

Best regards,

J.Ch.Bolomey
Professor, Unversity of Paris

Tel +33 01 69 85 15 41 / (15 42 Secr.)
Fax +33 01 69 41 30 60
Email bolomey@supelec.fr

Sensor and Simulation Notes

Note 417

9 January 1998

Spherical Near-Field Facility for Microwave Coupling Assessments in the 100 MHz - 6 GHz Frequency Range

D.Sérafin (+), J.L.Lasserre (+), J.Ch.Bolomey (*)
G.Cottard (°), Ph.Garreau (°), F.Lucas (°), F.Thérond (°)

Abstract

This paper describes a spherical Near-Field facility, set up at the Centre d'Études de Gramat, to perform low power microwave coupling assessments. Specifically, this facility has been designed to determine the Coupling Cross Section of a complex object. However, it can also be used for the characterization of any radiating system in Electromagnetic Compatibility (EMC) or High Power Microwave (HPM) environments. The Near-Field approach is shown to offer complementarity and increased flexibility when compared to other more conventional measurement techniques. More particularly, the use of a probe array in the upper part of the frequency band significantly speeds up the Near-Field measurement process. Consequently, broadband and multiparameter acquisitions can be performed within acceptable duration. The examples given in this paper provide a broad illustration of the capabilities of Near-Field techniques for EMC and HPM applications.

(+) CEG (Centre d'Études de Gramat), DGA/DRET, F-46500 Gramat, France
(*) Supélec, Electromagnetics Department, Plateau de Moulon, F-91192 Gif sur Yvette, France
(°) Satimo (Société d'Applications Technologiques de l'Imagerie Micro-Onde), Rue Terre de Feu, F-91952 Courtaboeuf, France

1. Introduction

The penetration of an electromagnetic wave in electronic equipment is achieved via both antennas (front door coupling) and shielding defects (back-door coupling) such as apertures, connectors, seams, electrical discontinuities, etc... Front-door coupling is quite easy to predict via numerical modeling, especially in the operating frequency band of the antennas. On the contrary, back-door coupling, which involves complex out-of-band coupling mechanisms, is much more difficult to model numerically and requires extensive experimental assessments.

Such microwave coupling assessments involve specific instrumentation. Indeed, as is now well-known, CCS's in the microwave frequency range are very sensitive to parameters such as attitude (or incidence) angle, frequency and polarization. Accordingly, before conducting lengthy high power testing, a careful identification of the most critical operational conditions is of prime importance. Indeed, limiting high power testing to these worst case agression configurations results in significant reduction of overall testing time. As shown in this paper, NF techniques prove very effective to identify these most critical configurations, from low power coupling measurements. A spherical NF facility, called SOCRATE, has been designed by Satimo, based on concepts developed at Supélec, and installed at CEG. This facility is primarily devoted to the High Power Microwave (HPM) program of CEG. The purpose of this paper is to illustrate the potentials of such a NF facility as follows. After a brief introduction of the CCS concept, the Socrate NF facility is described and its salient features are indicated. Then, the basic principles for deriving CCS from NF data are given and illustrated by selected examples. More generally, SOCRATE is shown to be an efficient and flexible tool for the characterization of antennas and components involved in HPM and, more generally, in EMC applications. Examples of such applications are presented for the sake of illustration. Finally, the specific advantages and limitations of the NF approach are discussed, by comparison with other, more conventional, techniques which are currently used to determine experimentally the CCS of complex objects.

2. The Coupling Cross Section concept

The CCS concept, defined for EMC or HPM configurations, derives directly from the absorption cross-section, which is widely used in the field of antennas practice. Indeed, in both cases, a cross-section $\sigma(M)$ is introduced to relate the coupled or received power W_r, to the incident power density

per surface unit P_{inc}. For a given terminal pair (A,B), located in the Object Under Test (OUT), the CCS is defined as follows (Figure 1):

$$W_r = \sigma P_{inc} \qquad (1)$$

Such a definition can be used to directly determine the CCS from the measurement of the power delivered to the load impedance Z_L, connected at the ports (A,B), for a given incident power density. In this direct approach, the OUT behaves like a receiving antenna and the load impedance plays the role of a receiver input impedance. However, a major difficulty consists in reproducing, as accurately as possible, the real threat. The simulation of a plane wave, especially in the case of large objects, is usually not an easy task and supposes that parasitic interactions with the environment have been controlled and maintained below an acceptable level. Moreover, the possibility of modifying the attitude and polarization of the incident wave is usually severely limited in most existing simulators,by the ground plane, for instance .

Another indirect measurement scheme can be considered, where the OUT is now viewed as a transmitting antenna (Figure 2). Driven by an internal source connected at the ports (A,B), the object radiates, at a distance r and in the direction $\mathbf{u}$, a Far Field (FF) $\mathbf{E}(r,\mathbf{u})$ which can be written under this very general form:

$$\mathbf{E}(r,\mathbf{u}) = \mathbf{F}(\mathbf{u}) [\exp (-jkr)] / r \qquad (2)$$

where $\mathbf{F}(\mathbf{u})$ is the vector radiation characteristic and $k = 2\pi / \lambda$ is the propagation constant in the medium surrounding the OUT, λ being the wavelength. Then, using the reciprocity theorem, the CCS in the direction $\mathbf{u}$ and for a given point, $\sigma(\mathbf{u})$, can be written, as a function of the characteristics of both the incident plane wave and the OUT, considered as a transmitting antenna [1,2,3]:

$$\sigma(\mathbf{u}) = \frac{\lambda^2}{4\pi} \rho_{load} \rho_{pol} (\mathbf{u}) G(\mathbf{u}) \qquad (3)$$

with:

a) ρ_{load}, the load factor, represents the relative matching between the equivalent load impedance Z_L, viewed from the test ports (A,B), with respect to the input impedance Z_i of the object under test, considered as a transmitting antenna:

$$\rho_{load} = 1 - \frac{|Z_i - Z_L^*|}{|Z_i + Z_L|}^2 \qquad (4)$$

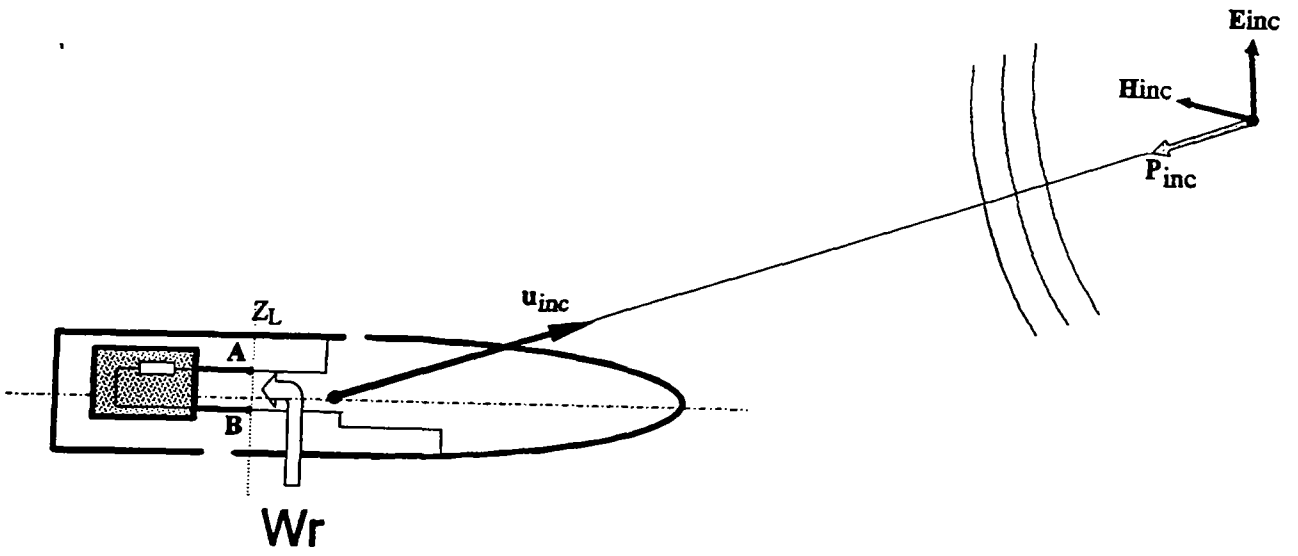

Figure 1: General configuration for the definition of the Coupling Cross-Section (CCS)

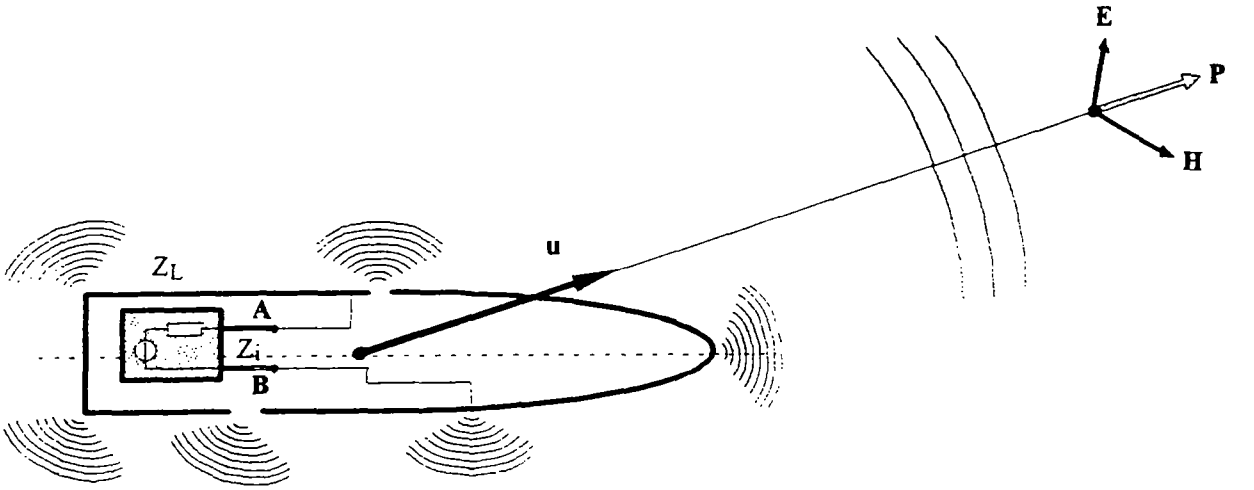

Figure 2: The reciprocal transmitting configuration associated with the coupling configuration depicted in Figure 1

The load factor is thus independent of both attitude and polarization. But it does depend however on the frequency and on the excited test point.

b) $\rho_{pol}(\mathbf{u})$, the polarization factor, depends on the normalized incident electric field $\mathbf{e}_{inc}$ and on the normalized FF radiation characteristic $\mathbf{f}(\mathbf{u})$ transmitted by the object under test:

$$\rho_{pol}(\mathbf{u}) = \left| \mathbf{e}_{inc} \cdot \mathbf{f}(\mathbf{u}) \right|^2 \tag{5}$$

where the normalized vector **a** associated with a complex vector **A** can be written by means of its norm $A' = (\mathbf{A} \cdot \mathbf{A}^*)^{1/2}$:

$$\mathbf{a} = \frac{\mathbf{A}}{A'} \tag{6}$$

c) $G(\mathbf{u})$ is the gain of the object under test, which can be expressed as a function of the normalized FF radiation characteristic:

$$G(\mathbf{u}) = 4\pi\chi \frac{f'^2(\mathbf{u})}{\int\int_{4\pi} f'^2(\mathbf{v})\, d\omega(\mathbf{v})} \tag{7}$$

where χ represents the radiation efficiency and $d\omega(\mathbf{v})$ denotes the element of solid angle in the direction **v**.

As compared to standard antenna problems, there are, for EMC or HPM applications, at least three major differences. First of all, the radiation efficiency χ can be very low for well hardened equipment. Secondly, the radiation characteristic **F** exhibits a large variability, in shape and levels, according to the frequency, the polarization and the attitude angle. Finally, the test frequency band must not only be dictated by the OUT properties, but also by the spectrum of the threat which may, generally, be very widely spread.

The polarization factor and the directivity both depend on the attitude angle **u**. Furthermore, the polarization factor also depends on the incident field orientation. Equation (3) clearly shows that the CCS depends on three primary parameters: 1) frequency, 2) attitude angle and 3) polarization. These dependences are explicitly shown on the flow chart given in Figure 3. Furthermore, equation (3) allows us to identify the quantities to be measured on the OUT, in order to determine the CCS. Namely, these quantities are the input impedance Z_i, the normalized FF radiation characteristic $\mathbf{f}(\mathbf{u})$ and the gain $G(\mathbf{u})$ of the OUT, considered as a transmitting antenna.

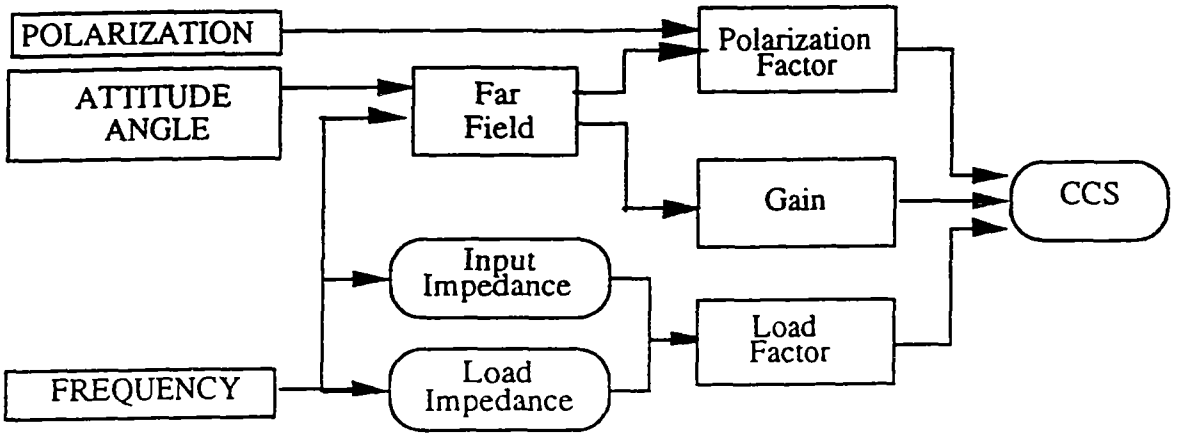

Figure 3: Flow-chart for a parametric analysis of the Coupling Cross Section (CCS)

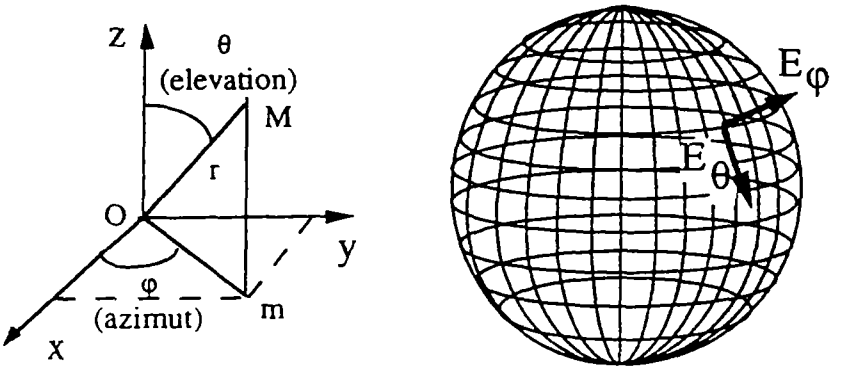

Figure 4 : The spherical coordinate system and the grid of the probing points on which the tangential components of the electric field are measured

Both **f(u)** and **G(u)** can be measured directly in the Far Field region, on a long range, or, equivalently, on a compact test range. However, these quantities can be also indirectly deduced by means of NF techniques. Such techniques consist of two steps, firstly the measurement of the NF distribution around the object under test and secondly, the calculation of the Far Field, via so-called Near Field to Far Field transformations.

3. The SOCRATE Near-Field facility

The SOCRATE NF facility has been designed to perform NF measurements in spherical coordinates. Unlike planar or cylindrical probing geometries used for high directivity telecommunication or radar antennas, the spherical geometry accommodates poorly directive objects radiating in a wide and rather unpredictable angular range, such as those involved in microwave coupling. The SOCRATE NF facility covers the frequency range extending from 100 MHz to 6 GHz. Indeed, initially designed for the 100 MHz - 4 GHz frequency band, the equipment has been shown to be able to operate up to 6 GHz with slightly degraded performances and smaller OUT's. The acquisition of the NF distribution over a sphere is achieved by combining a rotation of the test object on a turntable and NF measurements performed on a semi-circular 2 meter radius arc. At each probing point on the sphere, corresponding to given elevation (θ) and azimuth (φ) angles, both tangential components E_θ and E_φ are measured (Figure 4). The probe equipment is located in a large rectangular anechoic chamber (10m x 10m x 8m). Figure 5 shows a photograph of the measurement facility, a missile head being installed as OUT.

The frequency range is subdivided into two sub-bands, for which different measurement techniques are employed, as shown on Figure 6. The Low Frequency Band (LFB) extends from 100 MHz to 1 GHz. The measurements are performed by means of a broad band dual-polarized probe consisting of two resistively loaded crossed dipoles, 40 centimeters in length (Figure 7). This probe is mechanically displaced on the semi-circular arc. Due to the presence of the OUT positioner, there is a 14° blind angle, and the effective angular range covered by the probe is 0° to 166° on the θ angle. The outputs of the probe are directly connected to a HP-8510 Automatic Network Analyser (ANA) via a 20 meters long low loss cable. In the High Frequency Band (HFB), which extends from 1 GHz to 6 GHz, measurements are performed with a semi circular array of 128 dual polarized probes.

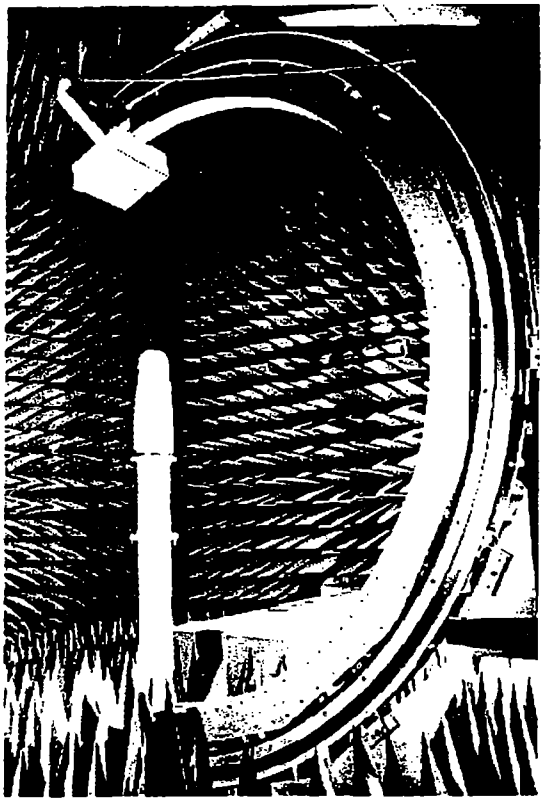

Figure 5: Overall view of the SOCRATE facility showing a missile head under test

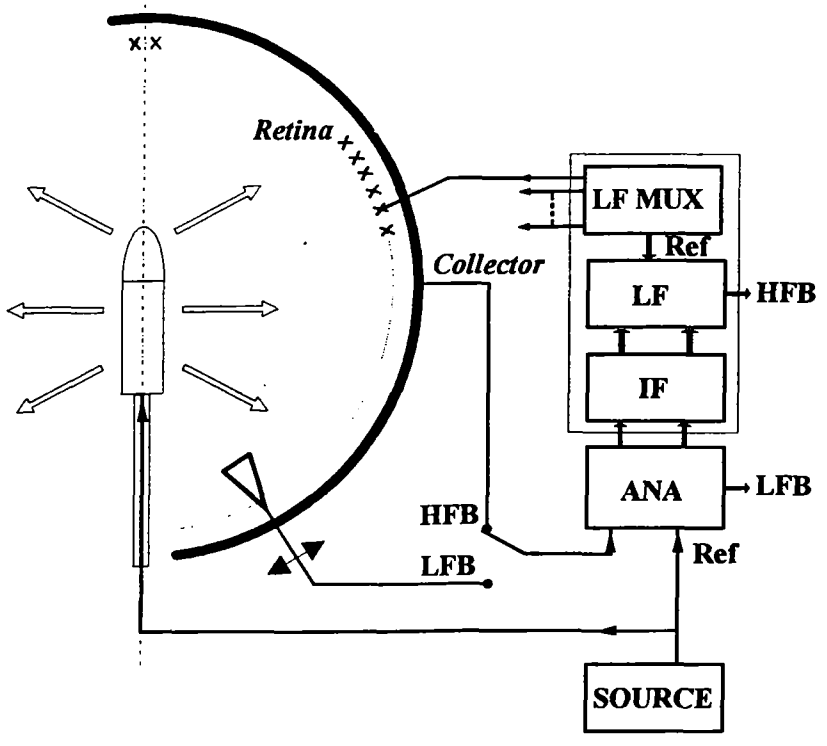

Figure 6: Block diagram organization of the SOCRATE facility

The design of the probe array is based on the so-called Modulated Scattering Technique (MST) [4,5,6,7]. The Near Field probing device consists of an array of small crossed dipole probes, called the retina, located in front of a collector antenna. The collector antenna consists of an array of 64 wide-band spiral antennas which are connected to the receiver via power splitters. The array is formed by 8 modules of 16 pairs of small crossed dipoles (Figure 8). Each dipole of the retina is loaded by PIN diodes. Modulating the diodes of a dipole results in a modulated signal at the output of the collector antenna. This modulated signal can be shown to be directly proportional to the field component at the corresponding probe location. Sequential addressing of the modulation to each element of the array provides a rapid way to record the NF distribution along the array. Such a recording process is time and cost effective: any mechanical motion of the probe is avoided, and no complex and expensive microwave multiplexer is needed to connect the different probes to the receiver. The blind angle for the HFB is only 5°, allowing for effective probing over 175° on the θ angle. Standard network analysers cannot be used directly with MST. Their final bandwidth (about 1 kHz) is too narrow when compared to the frequency of the modulation signal (about 100 kHz). For this reason, the reference and test outputs at the first Intermediate Frequency (IF) (20 MHz) of the network analyser are directed to an IF vector voltmeter. A LF synchronous detector at the modulation frequency provides the real part and the imaginary part of the electric field. These signals are then processed by a PC computer. The dispersion of probe response and the cross-polarization coupling between dipoles are compensated via a preliminary orthomodal calibration procedure [12].

4. CCS derivation from NF data in the SOCRATE facility

The flow-chart to derive CCS from measurements performed in the SOCRATE facility is shown in Figure 9. Input and load impedances are measured with a standard network analyser used in reflection mode. Knowledge of the object's input impedance and of the load impedance enables the calculation of the load factor from equation (4). The NF data are transformed to FF data in spherical coordinates by means of the numerical code SPH, developed by Supélec [8], based on standard spherical wave function expansions [9]. The FF data thus allow us to calculate:

1) the polarization factor, for any incident electric field which can be introduced as a parameter,

2) the gain for any direction.

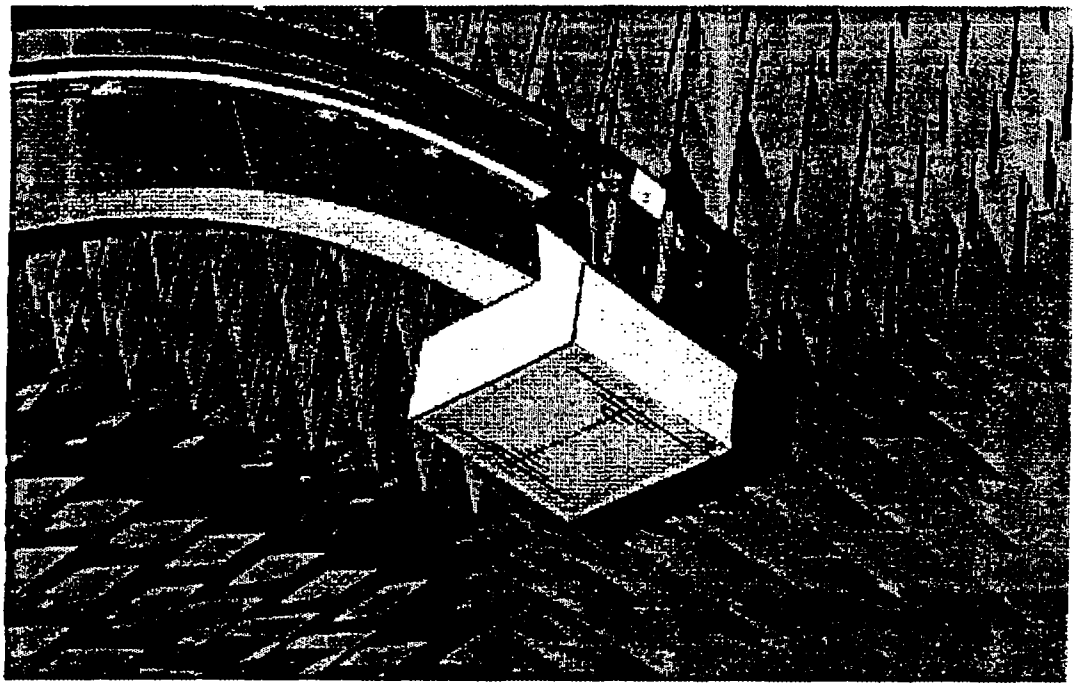

Figure 7: Dual-polarized crossed-dipole probe for LFB measurements (only one dipole is visible)

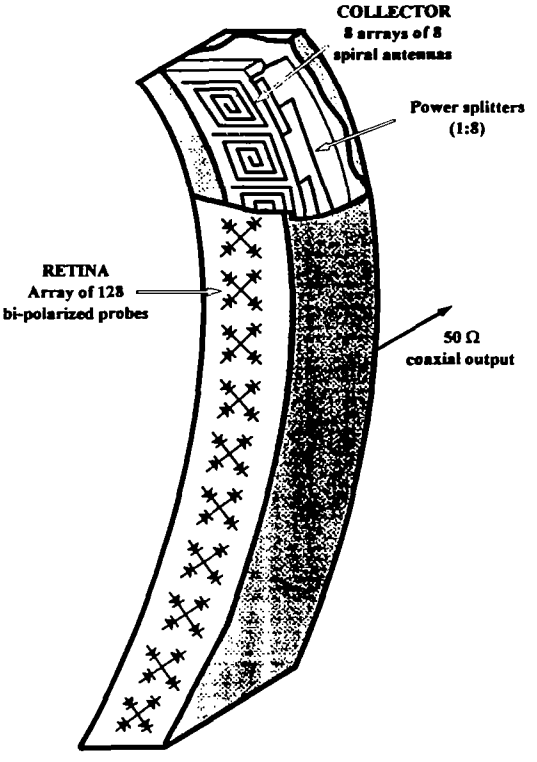

Figure 8: Schematic view of a module of the MST probe array for HFB measurements

Knowing the load factor, the polarization factor and the gain, the CCS can be derived for any attitude angle and any polarization. The time required to obtain CCS results depends primarily on the dimension to wavelength ratio of the OUT. Indeed, this ratio determines the number of measurements and, hence, the volume of data to be collected and processed. If R_{min} represents the minimum radius of the sphere inside which the object under test can be included, it can be shown that the total number of measurement points is given by N [9]:

$$N = 2 N_\theta (N_\theta - 1) \tag{8}$$

where the number of points in elevation, N_θ , is given by:

$$N_\theta = \frac{2 \pi R_{min}}{\lambda} + N_0 \tag{9}$$

and N_0 is of the order of 10 when N_θ is low; $2(N_\theta - 1)$ is the number of points along the azimuth angle φ. Figure 10 gives the number N_θ versus frequency between 100 MHz and 6 GHz, for R_{min} equal to 0.25 , 0.5 , and 1 meter, i.e., respectively for OUT length less than 0.5, 1, and 2 meters. In the LFB, the number of points in elevation can be arbitrarily chosen according to the OUT dimension, because the probe can be located at any point on the circular arc. In the HFB, this number is governed by the number of elements of the probe array, i.e., 128, which has been determined to provide suitable sampling at 4 GHz for a 2 meter long object. As a matter of fact, depending on the dimensions of the OUT, it is not necessary to take into account all of the measurement 128 points. For instance, in the lowest part of the HFB, one point out of two can be retained, or the measurements provided by adjacent probes can be spatially averaged, or, equivalently, several probes can be simultaneously modulated.

Figures 11a and 11b give the measurement time, on the basis of a single frequency analysis in the low (LFB) and high (HFB) frequency bands, respectively, with R_{min}= 0.5 meter. It is possible to estimate the time gain provided by the probe array over the single probe scan, when the frequency is increased. For example, the equivalent measurement time, at one frequency and with a single probe, would be 3 hours at 6 GHz, while it is only around 6 minutes with the probe array.

In the case of broadband analysis, the frequency sweeping strategy differs in the LFB and HFB. In the LFB, the mechanical scan being relatively slow (as 4°/second), as usual in single probe measurements, the frequency scan is performed for each measurement point. Typically, 40 ms are required to switch one frequency to another one.

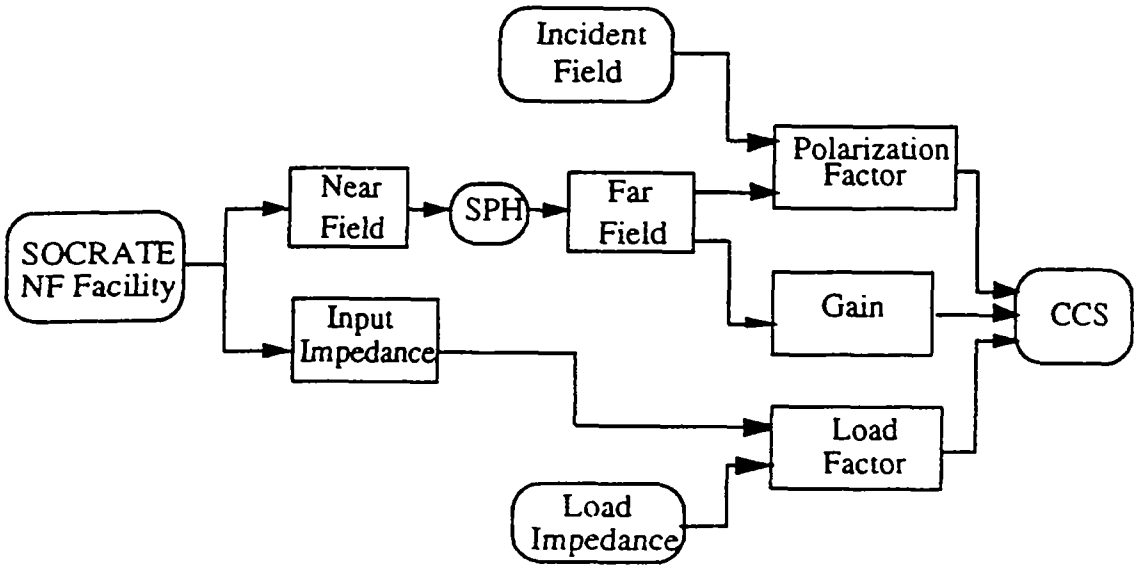

Figure 9: Flow chart to determine Coupling Cross Sections from Near Field measurements

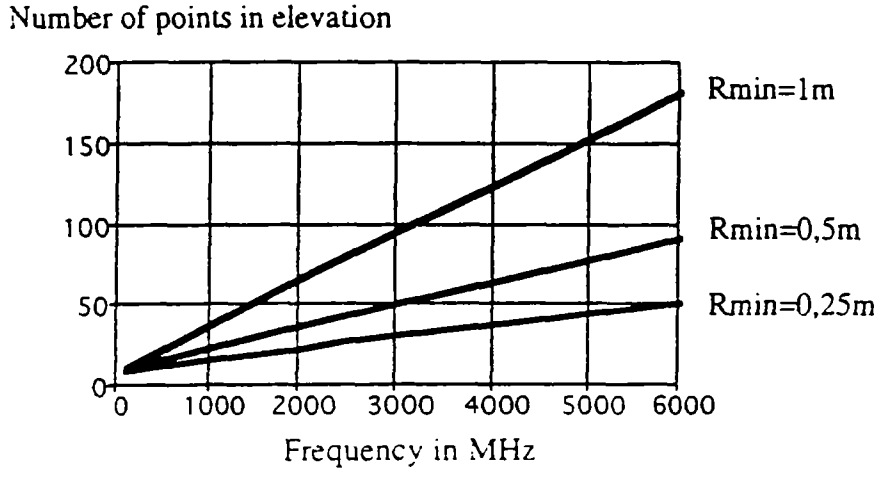

Figure 10: Number of points in elevation (N_θ) versus frequency, for different lengths of the object under test

On the contrary, in the HFB, the rapidity of the measurements (as100 to 1000 points per second, depending on the averaging) leads to the exploration of all the points at a given frequency, then, to switching the frequency. The advantage of the HFB strategy is that it enables NF to FF transformations to be started at a given frequency, without waiting for the overall frequency scan to be completed, as required for the LFB strategy. Figure 12 gives the measurement time in the case of a broad frequency band analysis extending from 100 MHz to 4 GHz, and involving 391 test frequencies corresponding to a frequency step equal to 10 MHz. As compared with fully mechanical measurements, it can be shown that the mixed mechanical (LFB) and electronic (HFB) scanning process used in SOCRATE provides a gain of more than 3 in the total duration of the NF measurements. These measurements are fully automated and can be performed 24 hours a day. To minimize the measurement duration, the best test parameters (gain, averaging, angular sampling interval, etc...) are self-controlled according to the frequency .

Figure 13 gives the time required to perform the NF to FF transformation by means of the numerical code SPH, on a 735 series HP9000 workstation, connected by a network to the PC computer driving the SOCRATE facility. NF to FF transformations, SEC calculations, as well as 3D plots are performed on this workstation. Temporary storage is performed on the 2 Gbytes hard disc of the workstation. The data are then compressed on optical discs (1.2 Gbyte) or digital audio tapes (DAT) (1 Gbyte) with a compression rate of about 70%. After compression, the NF and CCS data corresponding to 1 test point of a 1 meter long object, in the 100 MHz - 4 GHz frequency band with 10 MHz frequency step, typically require about 40 Mbytes. Consequently, up to 25 test points may be stored on a single DAT.

Finally, it is worth mentioning that the SOCRATE NF facility can be used even with non-reciprocal objects, involving, for instance, active devices. Insofar as reciprocity is invoked to derive equation (3), it could be thought that NF techniques only apply to reciprocal systems. However, the circuits and the probe array involved in SOCRATE are reciprocal, except for the source and some amplifiers which can be switched at low cost. Accordingly, the probe array can operate either in receiving mode, as implicitly assumed until now, or in transmitting mode. When the probe array operates in transmitting mode, the object under test is operating as a receiver. In this operating mode, a convenient weighted summation of the object response to each individually transmitting probe allows us to synthesize a plane wave response with arbitrary incidence angle. As a matter of fact, such a weighted summation is performed by the NF to FF transformation algorithm.

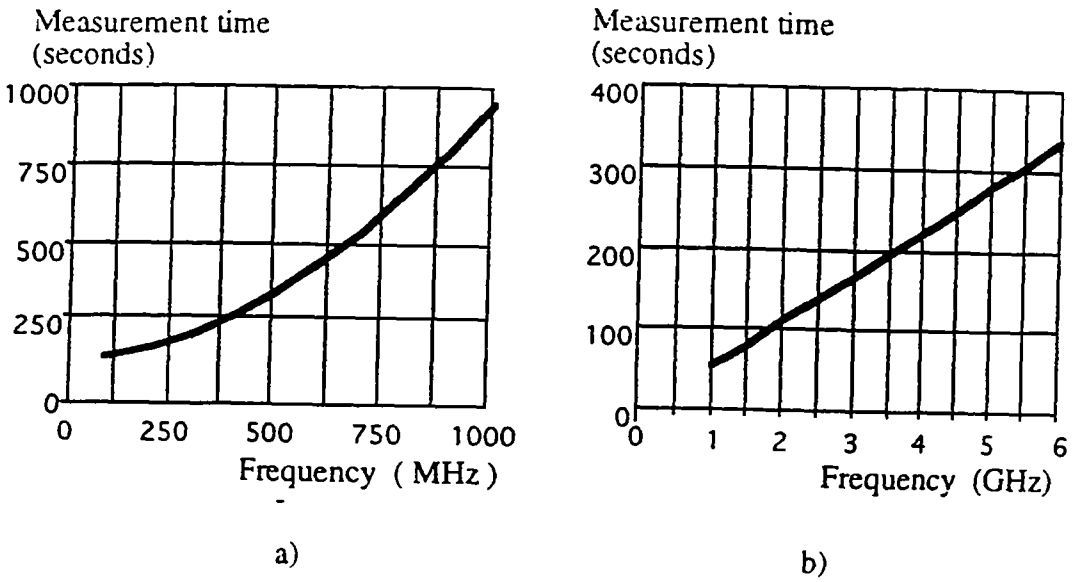

Figure 11 : Time of measurement for a 1 meter long object in the Low Frequency Band (LFB)[a], and in the High Frequency Band (HFB) [b], at one frequency

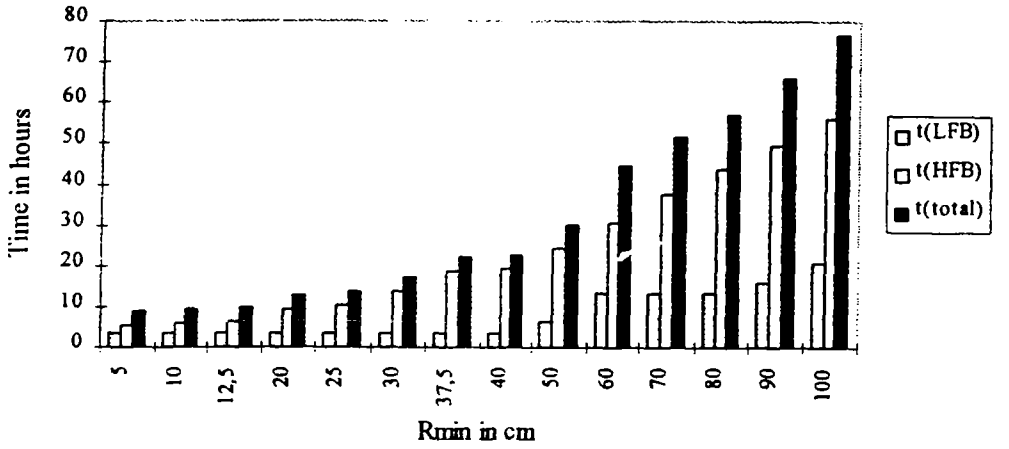

Figure 12: Total measurement time for an object in the 100 MHz - 4 GHz frequency band (391 frequencies) versus object length

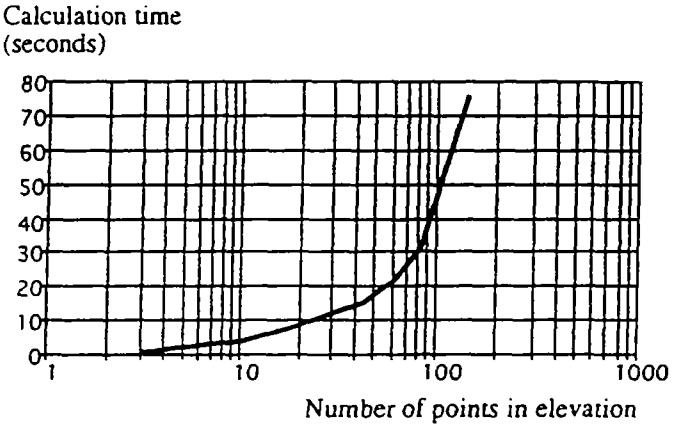

Figure 13: NF-FF transformation time versus the number of points in elevation N_θ

5. Results

The feasibility of determining CCS from NF data has been first investigated on generic objects with simple shape, consisting of a finite metallic cylinder with apertures on the walls (Figure 14). In the transmitting situation, the cylinder A (Figure 14.a) is fed by means of a vertical (parallel to z-axis) monopole antenna located inside the cylinder on its lower surface.

The results presented in Figures 15.a and 15.b show typical NF and CCS plots at 710 MHz from NF measurements performed on object A with the LFB arrangement (single probe). Object B was investigated with the HFB arrangement (probe array) at 2.165 GHz and 2.660 GHz.

Figures 16a.,16.b, 17.a and 17.b show NF and CCS plots at these two frequencies and illustrate, for this object, the extreme variability versus frequency and attitude angle.

An example of a more realistic test object is shown on Figure 18. This object is a missile head equipped with a radar for guidance purposes. The radar aperture is then expected to constitute a significant Port Of Entry (POE) with respect HPM beams. Figure 18.a and 18.b show the NF distribution and the CCS plot for a test point located in the missile head. Along with CCS measurements, the SOCRATE facility can be also used for other measurements of practical relevance in microwave coupling. For instance, NF to Very Near Field (VNF) transformations can be performed in order to identify and locate the POE's on the OUT [10]. Solving an inverse source problem allows us to retrieve, from the measured NF data, the equivalent current distribution on the OUT and, hence, to determine the position of the radiating apertures. As shown on Figure 18.c, the predominant role played by the radar antenna aperture has been confirmed by using this diagnostic technique. The area most actively contributing to the missile head CCS is clearly stemming from the top end radome region.

More generally, the SOCRATE facility is a very flexible tool to characterize, rapidly and accurately, any radiating element involved in microwave coupling experiments. As an example, the antennas devoted to HPM or EMC testing can be fully characterized from NF measurements. The NF distribution allows us to compute the radiated field at any distance larger than the radius R_{min} of the minimum sphere surrounding the antenna under test. Such a spatial characterization can be useful for many purposes.

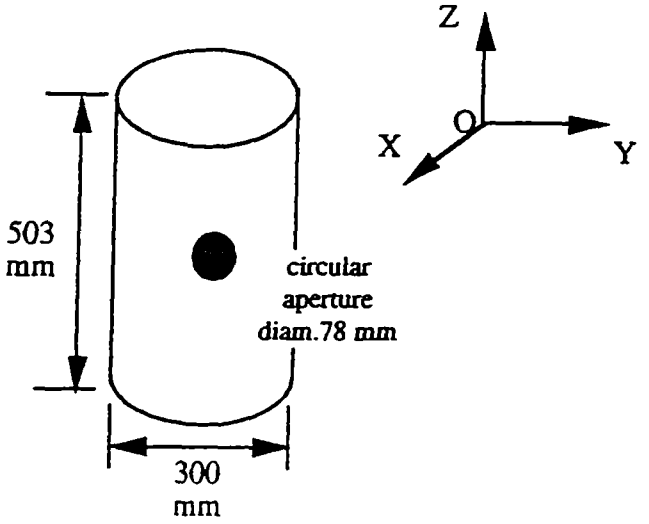

Object A

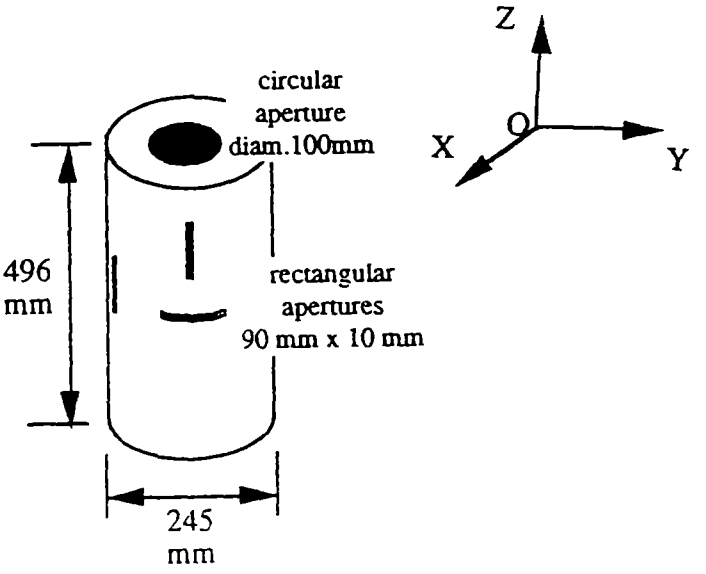

Object B

Figure 14: Generic objects A and B, with simple shape and apertures

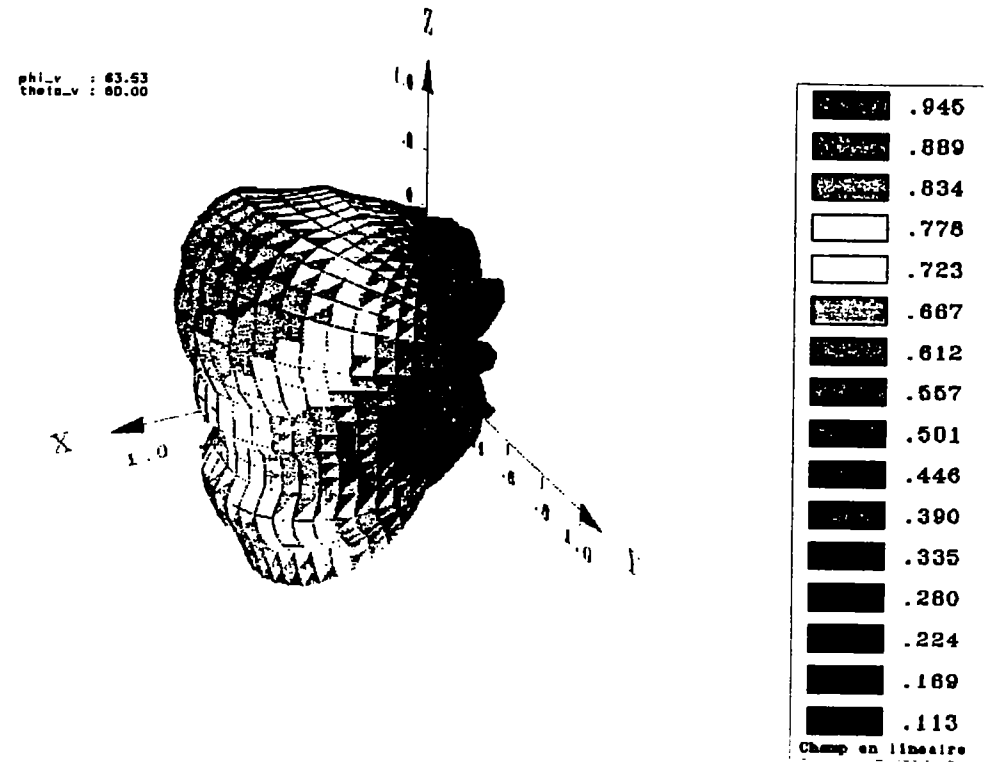

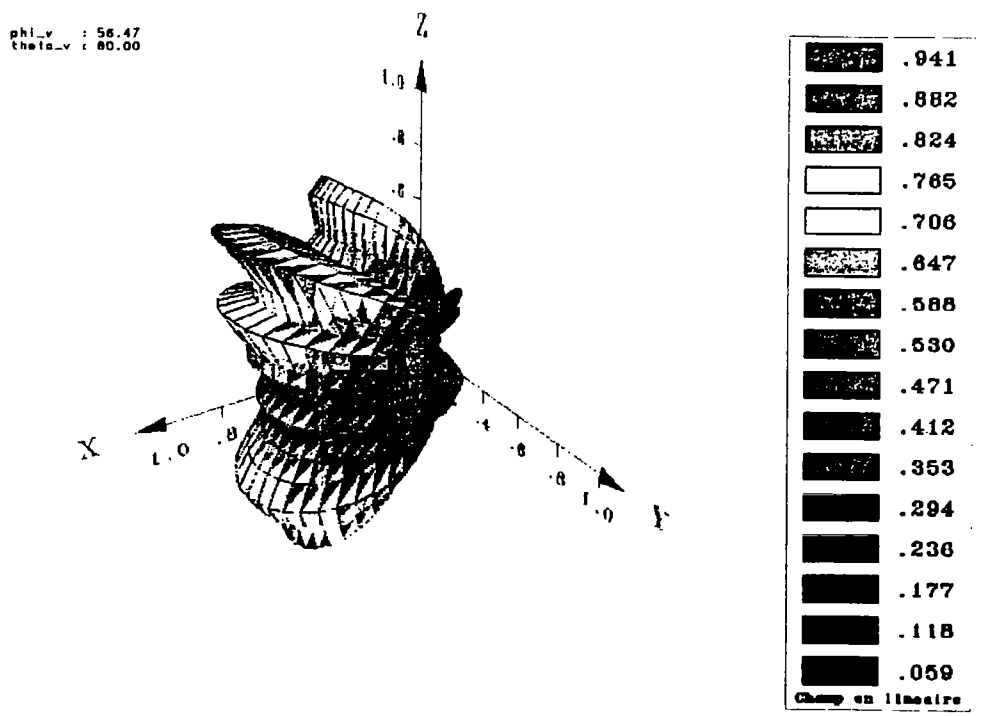

Figure 15 : NF distribution [a] and CCS plot [b] of object A at 710 MHz
(linear scale, arbitrary units, both co- and cross-polar contributions are included)

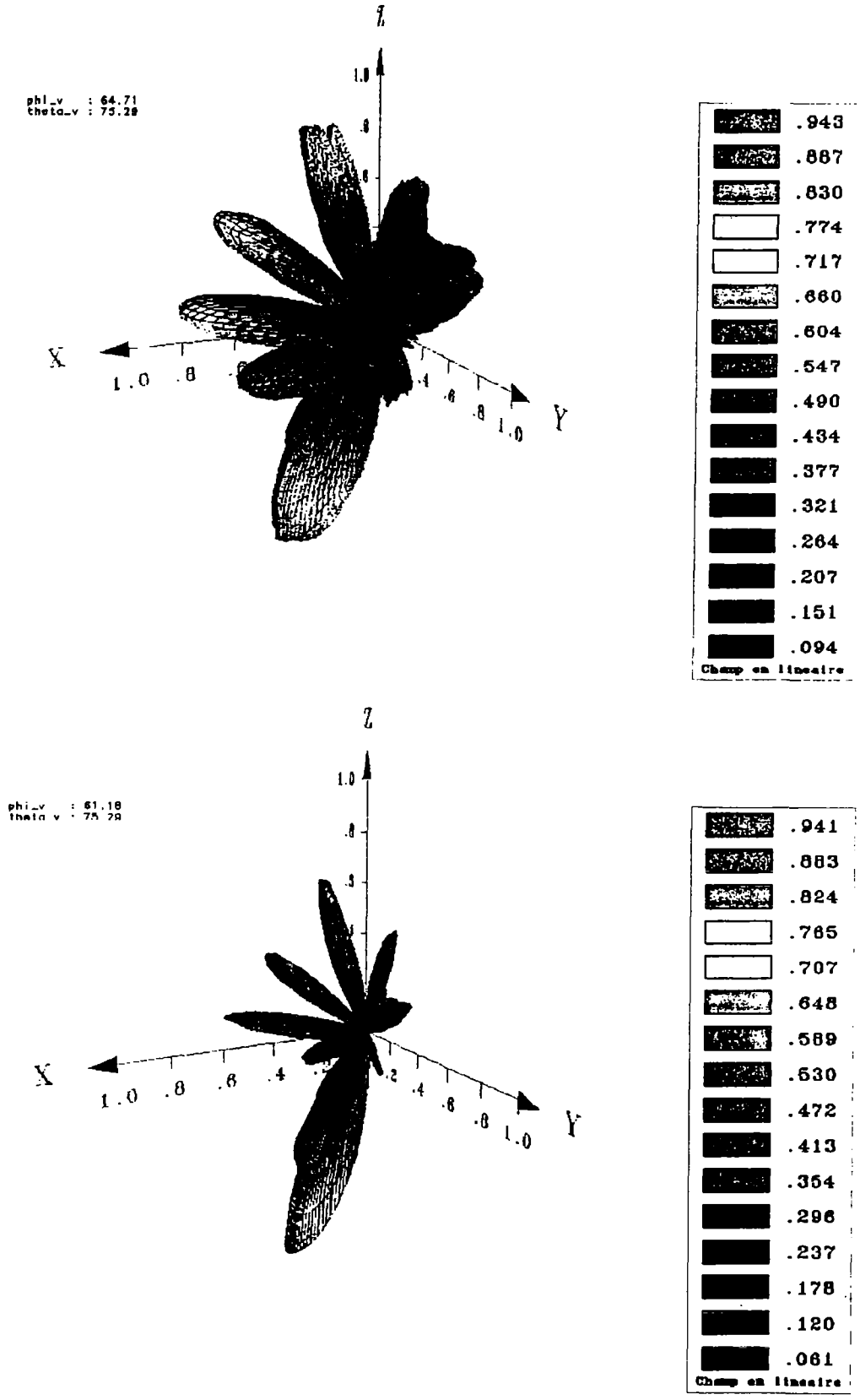

Figure 16 : NF distribution [a] and CCS plot [b] of object B at 2.165 GHz
(linear scale, arbitrary units, both co- and cross-polar contributions are included)

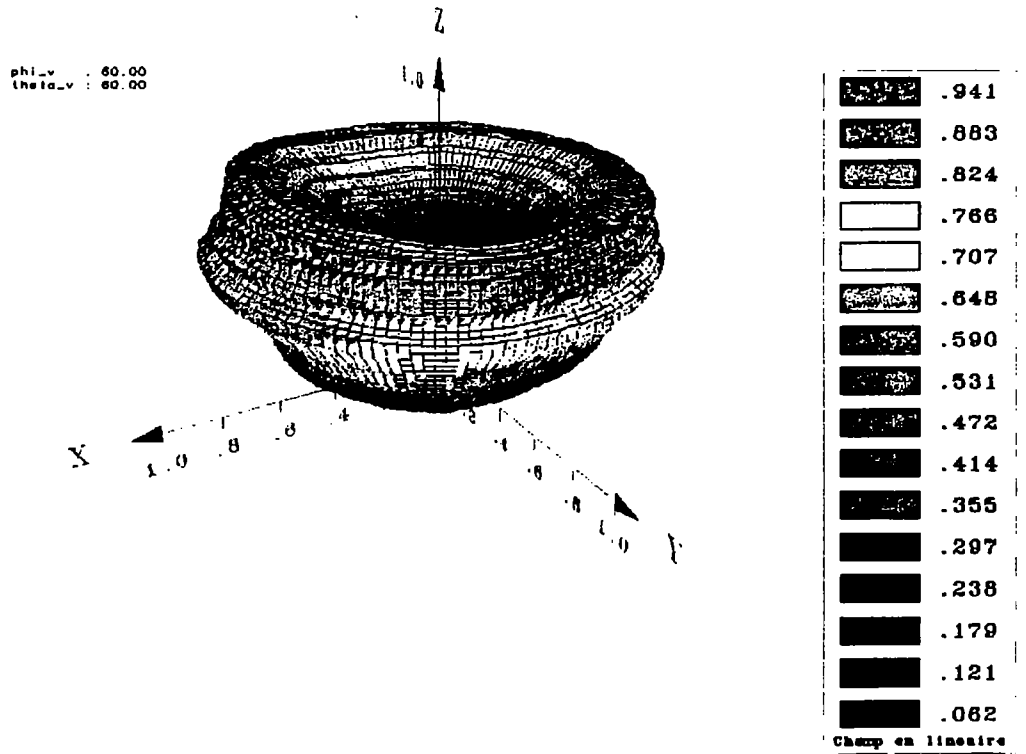

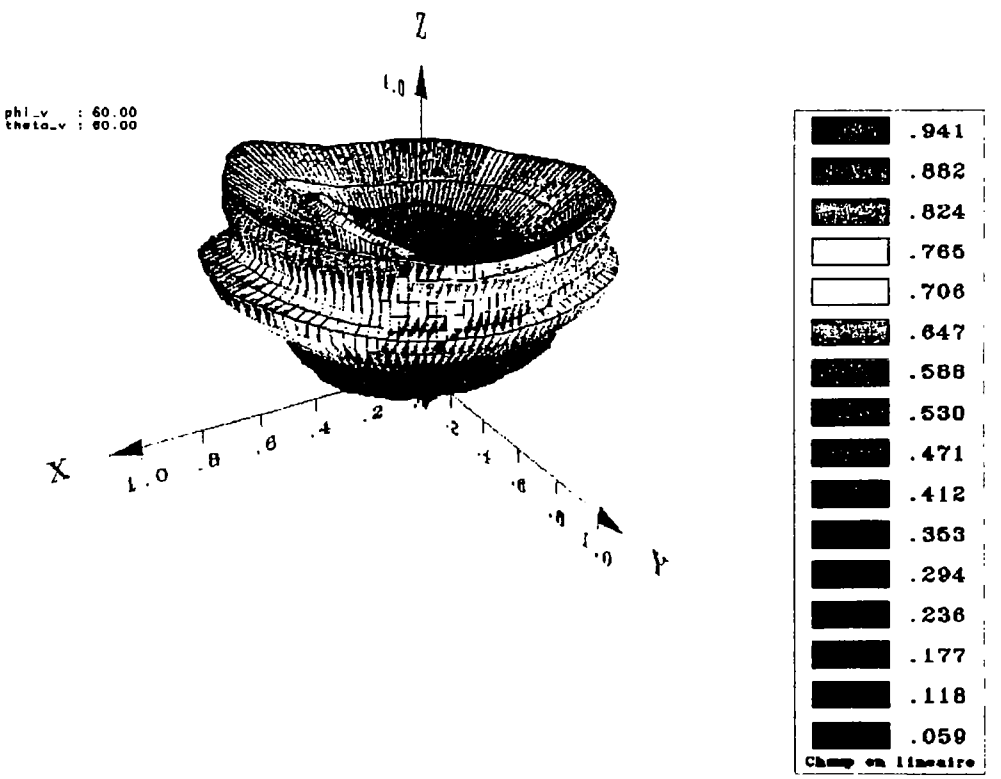

Figure 17 : NF distribution [a] and CCS plot [b] of object B at 2.660 GHz
(linear scale, arbitrary units, both co- and cross-polar contributions are included)

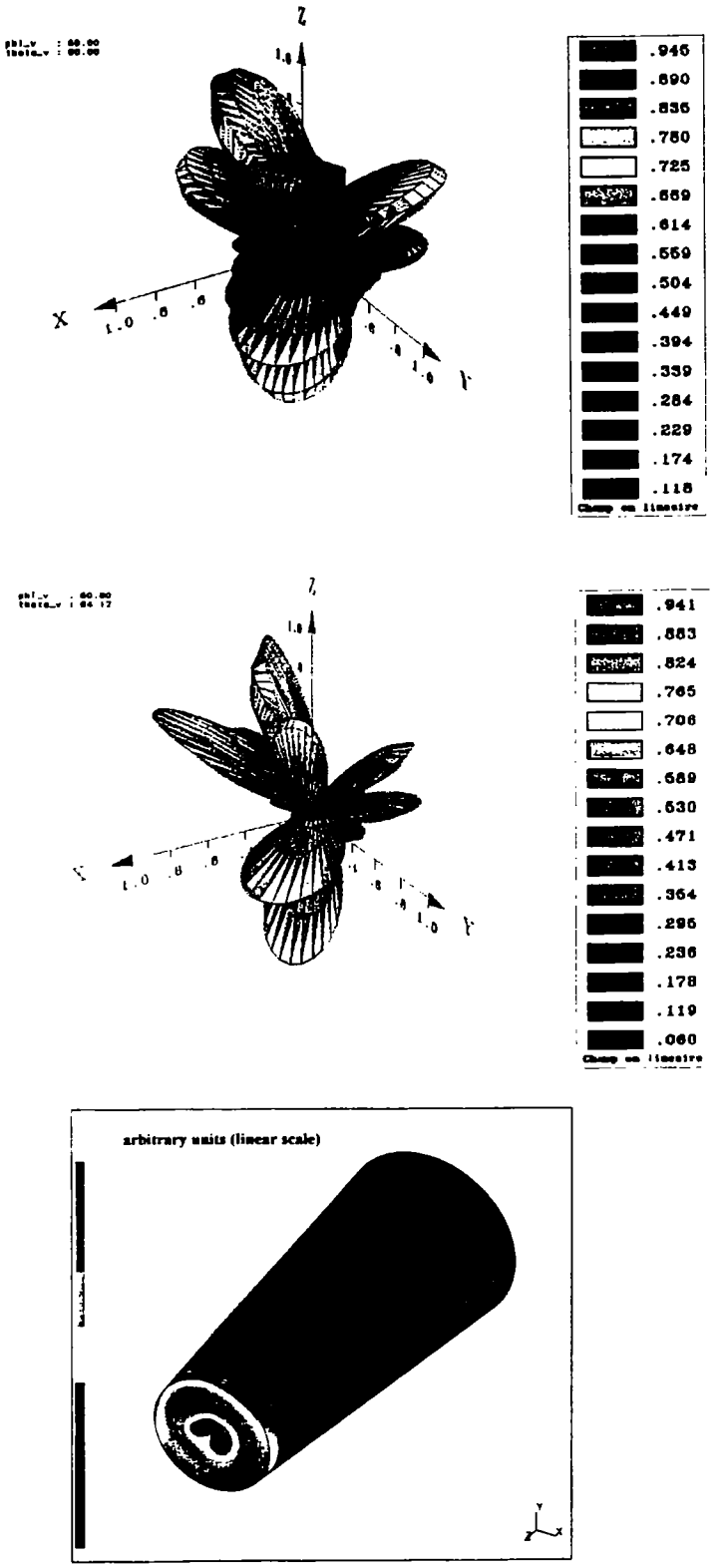

Figure 18: NF distribution [a] and CCS plot [b] of a missile head at 920 MHz , and location of the coupling aperture via an electromagnetic diagnostic procedure [c] (linear scale, arbitrary units, both co- and cross-polar contributions are included)

For example, some possible applications may consist 1) in determining the areas in MFP experimental setups exhibiting unacceptable hazardous parasitic radiation levels, 2) in estimating the effect, on the radiated field, of various devices introduced to maintain power handling requirements such as electromagnetic radomes or windows, 3) in assessing the coupling between the elements of radiating arrays or 4) in determining the NF distribution of primary feeds in view of optimizing the illumination of reflectors or periscopic systems to be used for producing collimated high power beams with large cross-sections.

6. Conclusion

The examples shown in this paper have been selected to illustrate the capabilities of NF approaches for HPM and EMC applications. They confirm the potentialities of these techniques when dealing with complex microwave coupling problems, which require the complete characterization of the objects under test [11]. Specifically, for HPM applications, these techniques enable the of the most critical coupling configurations and, consequently, it is possible to prepare subsequent high power testing more adequately. The SOCRATE NF facility has been shown to offer attractive performances in terms of rapidity, sensitivity and accuracy.

It can be operated over a wide frequency band 100 MHz - 6 GHz and has provided good results with objects exhibiting very low Coupling Cross-Section ($\approx 10^{-8}$ m^2), as well as with high gain ($\approx$ 20 or 30 dB) antennas. Measurement time is not a real limitation, even in the HFB, where the probe array solution gives high probing rates, up to 1,000 measurement points per second. Furthermore, via a convenient probe array design, the interaction between the experimental set-up and the object under test has been checked to be maintained at a sufficiently low level to guarantee convenient accuracy. Currently, assessments are conducted on missiles and equipment like GPS systems, and a research effort is devoted to CCS analysis in order to define appropriate hardening techniques to obtain adequate protection of electronic systems against electromagnetic threats.

When compared other more conventional techniques, the NF approach avoids the simulation of a uniform plane wave incident field on the OUT, with variable incidence angle and polarization. One set of measurements performed in a transmitting situation is sufficient to predict the behaviour of the OUT in receiving situations for any plane wave incidence angle and polarization. Furthermore, the

OUT response to an arbitrary incident field can de deduced from the knowledge of the plane wave response, via an angular plane wave spectrum expansion of the incident field. More particularly, the NF data can be used to yield averaged results, such as those provided by reverberating chambers. The NF approach shares with other techniques the difficulties associated with access to the test point. Indeed, the connection of a cable to a given point located inside a piece ofequipment is known to be difficult or even impossible in some cases. The problem is simpler for prototypes. The NF approach can be used for non-reciprocal objects. It is worth pointing out that, in the transmission mode, the need for delivering some power to the equipment has not proven to be a major limitation. Typically, transmitted power ranges between 0.01 mW and 10 mW, according to the radiation efficiency of the OUT. An optical link is now available in the transmitting mode for minimizing parasitic interactions between the OUT and conventional coaxial cable feeding. Such a link has been shown to be particularly useful for reliable measurements, especially on small OUT such as portable communication systems [13].

References

[1] J.Brown, "A Generalized Form of the Aerial Reciprocity Theorem", Proc.IEE (UK), vol.103-c, n°4, 1-4, April 1958

[2] A.T. de Hoop, G. de Jong, "Power Reciprocity in Antenna Theory", Proc.IEE (UK), vol.121, n°10, 1051-1056, Oct.1978

[3] R.E.Collin, in "Antenna Theory", R.E.Collin and F.J.Zucker Ed., Chap.4, 93-117, Mac Graw Hill, New York, 1969

[4] J.H.Richmond,"A Modulated Scattering Technique for Measurement of Field Distribution" IRE Trans. MTT-3,13-17, 1955

[5] R.King,"Microwave Homodyne Sytems", IEE EM Wave Series Vol.3, Peter Peregrinus Ltd, Herts (UK), 1985

[6] J.Ch.Bolomey, "La méthode de diffusion modulée: une approche au relevé des cartes de champs micro-ondes en temps réel", L'Onde Électrique (F), vol 62, n°5, 73-78, Mai 1982

[7] J.Ch.Bolomey, B.J Cown, G Fine et al.,"Rapid Near-Field Antenna Testing via Arrays of Modulated Scattering Probes", IEEE Trans. AP-36, 804-814, June 1988

[8] G.Fine, J.Y.Gautier, J.Ch.Bolomey, J.Y.Gautier "SPH: Logiciel de transformation Champ proche / Champ lointain en coordonnées sphériques", Rapport final Lot 2, Contrat CEG N°418/110/01, Supélec, Gif sur Yvette (F), Sept. 1991

[9] J.Hansen,"Spherical Near-Field Antenna Measurement", IEE EM Wave Series Vol.26, Peter Peregrinus Ltd, Herts (UK), 1988

[10] F.Thérond, J.Ch.Bolomey, N. Joachimowicz, F.Lucas,"Electromagnetic Diagnosis Technique Using Spherical Near-Field Probing", in Electromagnetic Environments and Consequences, Proc.EUROEM'94, vol.2, chap.12,1218-1226, D.Sérafin et al. Ed., CEG, Gramat (F) 1995

[11] J.Ch.Bolomey,"Rapid Near-Field Techniques for EMC Applications", Proc.10th Int.Symp. EMC Zürich, Zürich (CH), 9-11March 1993, 55-60

[12] Ph.Garreau, F.Lucas, J.Ch.Bolomey, "Orthomodal Transducer Implementation for Antenna Measurement System", Proc.3rd International Workshop on Radar Polarimetry, Nantes (F), 21-23 March 95, p.267

[13] J.L.Lasserre, D.Sérafin, J.Ch.Bolomey, F.Lucas, F.Thérond, "Characterization of Portable Communication Systems by Means of Near-Field Techniques", in Wireless Communications, J.J.Pan Editor, SPIE Proc.Series, vol.2556, 50-58